

**Sharon Loh, BDS, FRACDS,  
MSc, MOrth RCS, MOrth RCS,  
FAMS**  
Registrar

**Mimi Yow, BDS, FDS RCS, MSc**  
Senior Consultant

Department of Orthodontics  
National Dental Centre  
Singapore

**Reprint requests:**

Dr Sharon Loh  
Department of Orthodontics  
National Dental Centre  
5, Second Hospital Avenue  
Singapore 168938  
Fax: +65-63248890

## Computer prediction of hard tissue profiles in orthognathic surgery

*The purpose of this retrospective study was to analyze the accuracy of computer predictions by CASSOS (Computer-Assisted Simulation System for Orthognathic Surgery) 2001 software (2000 SoftEnable Technology). Forty adult patients who had undergone orthognathic surgery were evaluated. Pre- and postsurgical lateral cephalographs were scanned into the computer, and 71 landmarks for each cephalograph were digitized. Digitization error was assessed from repeated digitizations. A customized cephalometric analysis consisting of 14 measurements was used in this study. Predicted and actual postsurgical hard tissue landmarks were compared using the Student t test. Results showed good correlation between repeated digitization for all measurements. There were no statistically significant differences in 10 of the 14 measurements. The differences that were statistically significant were in angular measurements for SNA angle, upper incisor to maxillary plane angle (U1-MxP), interincisal angle (U1-L1), and upper incisor to anterior cranial base angle (U1-SN). The greatest mean difference measured was the interincisal angle (U1-L1) which, although statistically significant, was clinically insignificant. This investigation showed that CASSOS 2001 software provides accurate hard tissue prediction for orthognathic surgical procedures. (Int J Adult Orthod Orthognath Surg 2002;17:342-347)*

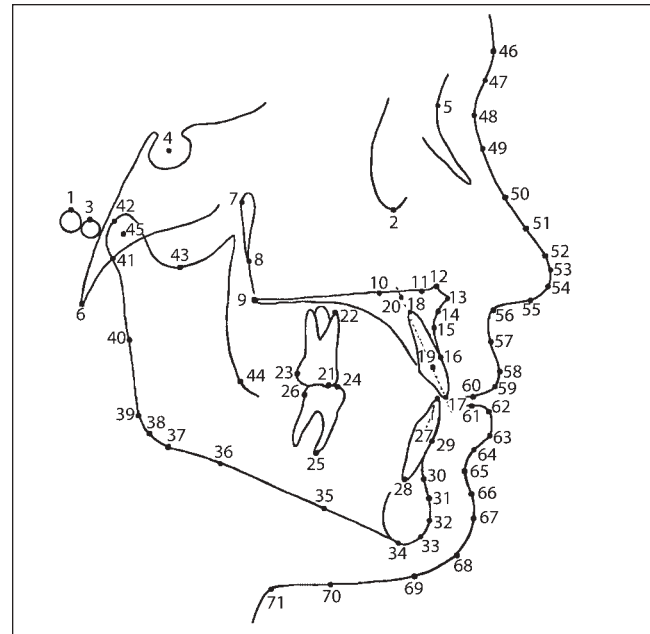
Orthognathic surgery is gaining popularity as the number of adults seeking orthodontic treatment increases.<sup>1</sup> Its popularity is also a result of greater predictability in its outcome. Many adults who seek such treatment would like to visualize the postsurgical result. Traditionally, orthognathic surgical planning involves clinical evaluation, photographs, freehand surgical simulation based on cephalometric tracings, and study model surgery.<sup>2-4</sup> However, this form of surgical planning does not allow patients to view the outcome easily, and often they cannot appreciate the final predicted result.

With the use of computers in orthognathic surgical planning, cephalometric tracing and surgical simulation can be done with ease, and superimposition of the tracings over the photographs allows the patient to quickly understand and ap-

preciate the final outcome. However, for computer prediction to be a useful clinical tool, it must be accurate, and the differences between the final result and the predicted outcome should be negligible.

Schendel et al<sup>5</sup> were probably the first to employ such a computer system for cephalometric analysis. Since then, this has become popular with many clinicians, as is evident by the vast number of software programs available on the market for cephalometric analysis as well as surgical prediction purposes. Such software also allows for diagnosis, treatment planning, and growth prediction.<sup>6-8</sup> Many clinicians have evaluated the accuracy of orthognathic surgical prediction based on cephalometric software. The results are encouraging. However, like manual cephalometric tracing, computer digitization is prone to errors.<sup>9,10</sup> It is helpful to recognize these errors so

**Fig 1** Location of cephalometric landmarks. Reproduced with kind permission of CASSOS 2001 software (2000 SoftEnable Technology). See "Landmarks used" list for definitions.



that they can be minimized and data analysis and interpretations will be meaningful for the clinician. This scientific tool is also useful in patient communication, since an accurate computer prediction allows the patient to have a more realistic expectation of the surgical outcome.

The aim of this retrospective study was to assess the accuracy of computer prediction by CASSOS (Computer-Assisted Simulation System for Orthognathic Surgery) 2001 software (2000 SoftEnable Technology). The investigation used computer predictions from presurgical lateral cephalographs, and comparisons were made with radiographs taken immediately postsurgery.

### Materials and methods

Forty adult orthognathic surgery patients from the National Dental Centre, Singapore, were used in this study. The sample consisted of 15 men and 25 women, with a mean age of 25 years (range, 16 to 45 years). All subjects had undergone 1 or a combination of the following surgical procedures:

1. Le Fort I maxillary impaction (18 subjects) or downfracture (6 subjects)
2. Le Fort I maxillary advancement (25 subjects) or setback (4 subjects)

3. Bilateral sagittal split osteotomy for advancement (7 subjects) or setback (28 subjects)
4. Genioplasty in combination with the above procedures (14 subjects)

Pre- and postsurgical lateral cephalographs were obtained on a Cephalostat (Soredex, Finndent). The patient's head was oriented in the natural head posture. The object-film distance was 20 cm and the cathode-object distance was 180 cm.

The presurgical lateral cephalographs were taken at a mean of 2 months (range 0.1 month to 7 months) prior to surgery. Postsurgical lateral cephalographs were taken at a mean of 4.7 days (range 3 days to 2 weeks) after surgery. The pre- and postsurgical lateral cephalographs were then digitized, using the CASSOS 2001 software, by 1 examiner.

The radiographic images were scanned prior to digitization. A transmissive scanner (Expression 1600 Pro, Epson) at 200 dots per inch was used to transfer the images into the CASSOS program. The digital radiographic images were then digitized using an on-screen digitizer. Seventy-one landmarks of both soft and hard tissue profiles were recorded for each cephalograph (Fig 1). A customized cephalometric analysis consisting of 14 measurements was used in this study (Table 1). Intraoperator error was

Landmarks used list	
1 = Porion (Po), most superior point of the external auditory canal (Anatomic Po); If Frankfort horizontal is constructed on machine Po (MaPo) and Orbitale, this landmark should be then digitized at MaPo's position, and overlapping on the landmark of MaPo	36 = Antegonion (AGo), a mid-planned point on the inferior border of the mandible at the depth of concavity of the antegonial notch
2 = Orbitale (Or), most inferior point on the infraorbital rim	37 = Inferior gonion (IGo), a mid-planned point at a tangent to the inferior border of the mandible near gonion
3 = Machine porion (MaPo), midpoint of the most superior contour of the metal ear rod of the cephalometer or cephalostat (machine porion), used for matching the color portrait to the radiograph	38 = Gonion (Go), a mid-planned point at the gonial angle of the mandible located by bisecting the posterior and inferior borders of the mandible
4 = Sella (S), midpoint of sella turcica, a constructed radiologic point in the median plane	39 = Posterior gonion (PGo), a mid-planned point at a tangent to the posterior border of the ramus gonion
5 = Nasion (N), junction of the frontal and nasal bones at the naso-frontal suture	40 = Posterior ramus (PR), a mid-planned point on the posterior border of the ramus, approximately halfway between gonion and articulare
6 = Basion (Ba), most inferior point on the anterior margin of foramen magnum, at the base of the clivus	41 = Articulare (Ar), a mid-planned point located at the intersection of the posterior border of the ramus with the inferior surface of the cranial base
7 = Pterygoid (Pt), landmark at 11 o'clock of the posterior shadow of pterygo-maxillary fissure, a bilateral teardrop-shaped area of radiolucency, the posterior of the shadow which represents the pterygoid plates, whereas the anterior shadow of which represents the posterior surfaces of the tuberosities of the maxilla	42 = Condylion (Co), the most posterosuperior point of the mid-planned contour of the mandibular condyle
8 = Pterygomaxillary fissure (Ptm), landmark at 6 o'clock position of the mid-planned contour of the pterygomaxillary fissure, at the junction of the pterygoid plates and the maxilla	43 = Sigmoid (Sg), a landmark at the deepest concavity of the mandibular sigmoid notch
9 = Posterior nasal spine (PNS), posterior limit of the floor of the nose, at the tip of the posterior nasal spine	44 = Anterior ramus (PtJ), a landmark at the deepest point of the curvature formed at the junction of the anterior portion of the ramus and the body of the mandible
10 = Anterior maxillary osteotomy point, landmark on the superior surface of the maxilla, delimiting posterior and anterior maxillary segments in segmental maxillary osteotomy simulations	45 = Center of the condyle (CC), a landmark representing the center of the rotation of the mandible, arguably the center of the head of the condyle
11 = Posterior nasal crest point (PNC), landmark on the superior surface of the maxilla before it turns upward to form the nasal crest	46 = Glabella (G), the most anterior point on the forehead, in the region of the supraorbital ridges
12 = Nasal crest point (NC), the most superior landmark on the superior surface of the maxilla which turns upward as it extends anteriorly, forming the nasal crest	47 = Superior soft tissue nasion (SNa), a landmark located halfway between glabella and soft tissue nasion
13 = Anterior nasal spine (ANS), the anterior limit of the floor of the nose, at the tip of the anterior nasal spine	48 = Soft tissue nasion (Na'), the point of deepest concavity of the soft tissue contour of the root of the nose, which overlays the naso-frontal suture
14 = Sub-ANS, point located on the anterior surface of the maxilla near ANS, at a point where its superoinferior thickness is 3 mm	49 = Inferior soft tissue nasion (INa'), a landmark located at the junction of the inferior limit of the concavity of soft tissue nasion and the dorsum of the nose
15 = Point A (A), the deepest point in the concavity of the anterior maxilla between the anterior nasal spine and the alveolar crest	50 = Nasal dorsum (IND), a landmark located approximately halfway from nasion to pronasale
16 = Prosthion (Pr), alveolar rim of the maxilla; the lowest, most anterior point on the alveolar portion of the premaxilla, in the median plane, between the central incisors	51 = Inferior nasal dorsum, a landmark located at the junction of the dorsum and tip of the nose
17 = Upper incisor tip (U1T), the tip of the crown of the upper central incisor	52 = Superior pronasale (SPn), a superior point on the tip of the nose
18 = Upper incisor apex (U1A), the root apex of the upper central incisor	53 = Pronasale (Pn), the most prominent point on the tip of the nose
19 = Inferior upper dentoalveolar (IUD) process, a landmark located midway between the labial and palatal dentoalveolar rims	54 = Inferior pronasale (IPn), an inferior point on the tip of the nose, as the top becomes confluent with columella
20 = Superior upper dentoalveolar (SUD) process, a landmark along the long axis of the dentoalveolar process, just underneath the palatal plane	55 = Columella (Cm), the most anterior point on the columella of the nose, representing the anterior delimiter of the nasolabial angle
21 = Upper molar crown (U6), the tip of the mesial cusp of the upper first molar	56 = Subnasale (Sn), a point at which the nasal septum merges with the upper cutaneous lip in the midsagittal plane
22 = Upper molar apex (U6MA), the apex of the mesial buccal root of the upper first molar	57 = Superior labial sulcus (SLs), the deepest point the concavity of the upper lip, midway between subnasale and labrale superius
23 = Upper molar distal (U6D), a landmark located at the most distal point of the upper first molar crown	58 = Labrale superius (Ls), a point indicating the mucocutaneous junction of the upper lip and philtrum
24 = Lower molar crown (L6D), the tip of the mesial cusp of the lower first molar	59 = Inferior labrale superius (ILs), a landmark on the upper lip located midway between labrale superius and stomion superius
25 = Lower molar apex (L6MA), the apex of the mesial root of the lower first molar	60 = Stomion superius (Stms), the most inferior point on the vermilion of the upper lip
26 = Lower molar distal (L6D), a landmark located at the most distal point of the lower first molar crown	61 = Stomion inferius (Stmi), the most superior point of the vermilion of the lower lip
27 = Lower incisor tip (L1T), the tip of the crown of the lower central incisor	62 = Superior labrale inferius (SLi), a landmark on the lower lip located midway between stomion inferius and labrale inferius
28 = Lower incisor apex (L1A), the root apex of the lower central incisor	63 = Labrale inferius (Li), the mucocutaneous border of the lower lip
29 = Infradentale (Id), the highest, most anterior point on the alveolar process, in the median plane, between the mandibular central incisors	64 = Inferior labrale inferius (ILi), a landmark located midway between labrale inferius and labiomental fold
30 = Point B (B), the deepest point in the concavity of the anterior mandible between the alveolar crest and pogonion	65 = Labiomental fold (Lf), the deepest point in the concavity between labrale inferius and the soft tissue chin
31 = Anterior genioplasty point (AGen), a point on the chin contour between point B and pogonion, which represents the anterior limit of a genioplasty osteotomy	66 = Inferior labiomental fold (ILf), a landmark located midway between labiomental fold and soft tissue pogonion
32 = Pogonion (Pog), the most anterior point on the bony chin	67 = Soft tissue pogonion (Pog'), the most anterior point on the soft tissue chin
33 = Gnathion (Gn), the most anteroinferior point on the bony chin, located by bisecting mandibular and facial planes	68 = Soft tissue gnathion (Gn'), the most anteroinferior point on the soft tissue chin
34 = Menton (Me), the most inferior point on the bony chin	69 = Soft tissue menton (Me'), the most inferior point on the soft tissue chin, in the region inferior to menton
35 = Posterior genioplasty point (PGen), a mid-planned point on the lower border of the mandible representing the posteroinferior limit of a genioplasty osteotomy	70 = Midcervical point (MPtc), a landmark located midway between soft tissue menton and cervical point
	71 = Cervical point (Ptc), the junction of the submental region and the neck

Table 1	Angular and linear cephalometric measurements
Measurement	
Angular (deg)	
1	SNA angle
2	SNB angle
3	ANB angle
4	SN-MxP (anterior cranial base to maxillary plane angle)
5	SN-MnP (anterior cranial base to mandibular plane angle)
6	MxP-MnP (maxillary-mandibular planes angle)
7	FMA angle (Frankfort-mandibular planes angle)
8	U1-MxP (upper incisor to maxillary plane angle)
9	L1-MnP (lower incisor to mandibular plane angle)
10	U1-L1 (interincisal angle)
11	U1-SN (upper incisor to anterior cranial base angle)
Linear	
1	LAFH (lower anterior facial height) (%)
2	Wits (Wits appraisal) (mm)
3	L1-APog (mm)
A= point A; B = point B ; L1 = lower incisor tip; MnP = mandibular plane; MxP = maxillary plane; N = nasion; Pog = pogonion; S = sella; U1 = upper incisor tip. See "Landmarks used" list for detailed definitions.	

Table 2	Intraoperator error based on repeated measurements
Variable	Correlation coefficient
SNA (deg)	0.87
SNB (deg)	0.79
ANB (deg)	0.96
SN-MxP (deg)	0.79
SN-MnP (deg)	0.86
MxP-MnP (deg)	0.88
FMA (deg)	0.73
U1-MxP (deg)	0.88
L1-MnP (deg)	0.88
U1-L1 (deg)	0.87
U1-SN (deg)	0.90
LAFH (%)	0.84
Wits (mm)	0.71
L1-APog (mm)	0.92
LAFH = lower anterior facial height. See "Landmarks used" list for detailed definitions.	

determined by redigitizing 10 cephalographs 1 week after initial digitization.

To determine the accuracy of the computer prediction, actual surgical movements carried out by the surgeons were entered into the treatment panel in the computer program. The computer then calculated the hard tissue changes using the CASSOS algorithm.

#### Statistical analysis

Cephalometric measurements between the computer-predicted and actual results were calculated and statistically evaluated. Means and standard deviations were determined for each angular and linear measurement. Intravariability correlation was used as an indicator of association between the predicted and actual values. The Student *t* test was used to calculate the statistical significance between the predicted and actual values. The level of statistical significance was established at  $P < .05$ . To determine intraoperator error, dual measurements were compared to derive a

correlation coefficient for each value. All statistical analyses were undertaken using Microsoft 4DExcel 2000.

## Results

Results of the intraoperator error analysis showed that all 14 measurements had good reliability (Table 2).

Comparison of the mean values from the prediction program with those from the postsurgical lateral cephalographs showed that all 14 measurements demonstrated a maximum disagreement of 3.7 degrees (interincisal angle, U1-L1). The Student *t* test showed that in 10 of the 14 measurements, there were no statistically significant differences in the mean value. However, statistically significant differences were found in the mean value for SNA angle ( $P = .02$ ), U1-MxP ( $P = .0005$ ), U1-L1 ( $P = .002$ ), and U1-SN ( $P = .0003$ ) (Table 3).

The intravariability correlation showed a strong correlation ( $r > 0.50$ ) between the predicted and actual values in 11 of the 14

Table 3		Means and statistical evaluation of predicted versus actual measurements			
Variable	Predicted mean	Actual mean	Predicted – actual	P value	Intravariabile correlation
SNA (deg)	85.9 ± 5.1	84.7 ± 4.5	1.2	.02*	0.71
SNB (deg)	81.9 ± 4.3	81.5 ± 3.7	0.4	.11	0.83
ANB (deg)	4.0 ± 3.1	3.2 ± 2.9	0.8	.05	0.54
SN-MxP (deg)	7.0 ± 3.7	6.9 ± 4.0	0.1	.40	0.49
SN-MnP (deg)	34.0 ± 7.3	33.9 ± 6.1	0.1	.46	0.84
MxP-MnP (deg)	27.0 ± 7.1	27.0 ± 5.8	0.0	.45	0.78
FMA (deg)	27.9 ± 6.6	27.8 ± 5.4	0.1	.43	0.75
U1-MxP (deg)	115.0 ± 8.1	111.9 ± 8.2	3.1	.0005***	0.76
L1-MnP (deg)	91.0 ± 7.7	89.2 ± 12.5	1.8	.12	0.59
U1-L1 (deg)	126.7 ± 9.4	130.4 ± 9.9	3.7	.002**	0.70
U1-SN (deg)	108.0 ± 8.5	105.0 ± 7.7	3.0	.0003***	0.39
LAFH (%)	58.6 ± 3.1	58.5 ± 2.9	0.1	.41	0.71
Wits (mm)	-4.1 ± 4.7	-5.3 ± 4.1	1.2	.07	0.22
L1-APog (mm)	2.8 ± 2.6	2.8 ± 2.3	0.0	.46	0.67

\* $P < .05$ ; \*\* $P < .01$ ; \*\*\* $P < .001$  (Student *t* test).  
LAFH = lower anterior facial height. See "Landmarks used" list for detailed definitions.

measurements (Table 3). Three measurements (SN-MxP, Wits, and U1-SN) showed weak correlations:  $r = 0.49$ ,  $r = 0.22$ , and  $r = 0.39$ , respectively.

## Discussion

The accuracy of the predicted hard tissue changes is important, as it has a concomitant effect on the predicted soft tissue changes. An accurate prediction gives the patient a more realistic image of the surgical outcome. This prevents any dispute that may arise as a result of differences between the patient's expectations and the surgical outcome. The accuracy of the prediction is also important in treatment planning, as it allows the clinician to assess the various treatment options.

An assessment of the predictive accuracy of the CASSOS program showed that in 10 of the 14 parameters studied, there were no significant differences between the predicted and actual values. The 4 parameters that showed statistically significant differences between the predicted

and actual values were SNA (1.2 degrees,  $P = .02$ ), U1-MxP (3.1 degrees,  $P = .0005$ ), U1-L1 (3.7 degrees,  $P = .002$ ), and U1-SN (3.0 degrees,  $P = .0003$ ). Three of these parameters involve angular measurements of the maxillary incisor, so the differences could be a result of the difficulty in identifying the apex of the maxillary incisor on the lateral cephalograph.<sup>9</sup> Although these parameters showed statistical significance, the interincisal angle demonstrated the greatest mean difference of 3.7 degrees, which is not clinically significant (the range of standard deviation for normal values of interincisal angle is 10 degrees). The magnitude of differences by digital tracing was less than the reported errors obtained in manual cephalometric tracings.<sup>9,10</sup>

This study compared favorably with the study reported by Loh et al,<sup>11</sup> which used the Quick Ceph program for prediction. The parameters used in that study were similar to the present study. They found that 4 out of 14 parameters had statistically significant differences, and only 1 parameter (Wits appraisal) showed clinical significant

inaccuracy. The study by Loh et al<sup>11</sup> was used for comparison, because in both studies the postsurgical radiographs were taken soon after the surgery (mean period of 4.7 days versus 1 day). Most studies that were reported used postsurgical radiographs taken long after surgery. They compared either hard and soft tissue prediction<sup>12</sup> or purely soft tissue prediction.<sup>13-15</sup> Bony and dental changes or relapses that were not induced by the surgery were disregarded. Postsurgical orthodontics also influenced the hard tissue changes. It is also important to allow for postsurgical soft tissue swelling to subside to ensure accurate assessment of soft tissue changes. One such study was done by Donatsky et al,<sup>16</sup> who reported that computerized cephalometrics using the TIOPS system provided an accurate hard tissue prediction for the surgical procedure. However, the postoperative radiographs were taken 4 weeks postoperatively. As such, postsurgical soft tissue evaluations and predictive soft tissue facial outcomes were not assessed in that study.

More recently, Xia et al<sup>17,18</sup> have reported on 3-dimensional virtual-reality surgical planning and soft tissue prediction for orthognathic surgery. Although this form of simulation allows the final result to be viewed in all 3 dimensions, its accuracy has yet to be evaluated and proven. Presently, the use of lateral cephalographs for analysis and surgical prediction of outcome is still an accurate and useful tool for orthognathic surgical planning and predictions in the anteroposterior view. Cephalometric data is well established universally and is easily processed. Digital cephalometrics and transformation in surgical simulations as predictive measures are validated by this study.

## References

1. Nattrass C, Sandy JR. Adult orthodontics. *Br J Orthod* 1995;22:331-337.
2. Neubert J, Bitter K, Somsiri S. Refined intraoperative repositioning of the osteotomized maxilla in relation to the skull and TMJ. *J Craniomaxillofac Surg* 1988;16:8-12.
3. Satrom KD, Sinclair PM, Wolford LM. The stability of double jaw surgery. A comparison of rigid versus wire fixation. *Am J Orthod Dentofac Orthop* 1991;99:550-563.
4. Vig KD, Ellis E. Diagnosis and treatment planning for the surgical-orthodontic patient. *Dent Clin North Am* 1990;34:361-384.
5. Schendel SA, Eisenfeld J, Bell WH, Epker BN. Superior repositioning of the maxilla. Stability and soft tissue osseous relations. *Am J Orthod* 1976;70:663-674.
6. Ricketts RM. The evolution of diagnosis to computerized cephalometrics. *Am J Orthod* 1969;55:795-803.
7. Ricketts RM, Bench R, Hilgers JJ, Schulhof R. An overview of computerized cephalometrics. *Am J Orthod* 1972;61:1-28.
8. Ricketts RM. Perspective in the clinical application of cephalometrics. *Angle Orthod* 1981;51:115-150.
9. Baumrind S, Frantz RC. The reliability of head film measurements. 1. Landmark identification. *Am J Orthod* 1971;60:111-127.
10. Baumrind S, Frantz RC. The reliability of head film measurements. 2. Conventional angular and linear measurements. *Am J Orthod* 1971;60:505-517.
11. Loh S, Heng JK, Ward-Booth P, Winchester L, McDonald F. A radiographic analysis of computer prediction in conjunction with orthognathic surgery. *Int J Oral Maxillofac Surg* 2001;30:259-263.
12. Gerbo LR, Poulton DR, Covell DA, Russel CA. A comparison of a computer-based orthognathic surgery prediction system to postsurgical results. *Int J Adult Orthod Orthognath Surg* 1997;12:55-63.
13. Cszaszar GR, Bruker-Cszaszar B, Niederdelmann H. Prediction of soft tissue profiles in orthodontic surgery with the Dentofacial Planner. *Int J Adult Orthod Orthognath Surg* 1999;14:285-290.
14. Hing NR. The accuracy of computer-generated prediction tracings. *Int J Oral Maxillofac Surg* 1989;18:148-151.
15. Mankad B, Cisneros GJ, Freeman K, Eisig SB. Prediction accuracy of soft tissue profile in orthognathic surgery. *Int J Adult Orthod Orthognath Surg* 1999;14:19-26.
16. Donatsky O, Hillerup J, Bjorn-Jørgensen J, Jacobsen PU. Computerized cephalometric orthognathic surgical simulation, prediction and postoperative evaluation of precision. *Int J Oral Maxillofac Surg* 1992;21:199-203.
17. Xia J, Samman N, Yeung RW, et al. Three-dimensional virtual reality surgical planning and simulation workbench for orthognathic surgery. *Int J Adult Orthod Orthognath Surg* 2000;15:265-282.
18. Xia J, Samman N, Yeung RW, et al. Computer-assisted three-dimensional surgical planning and simulation. 3D soft tissue planning and prediction. *Int J Oral Maxillofac Surg* 2000;29:250-258.